Soil Biology and Biochemistry 189 (2024) 109259

Contents lists available at ScienceDirect

Soil Biology and Biochemistry

journal homepage: www.elsevier.com/locate/soilbio

A pulse of simulated root exudation alters the composition and temporal dynamics of microbial metabolites in its immediate vicinity

Julia Wiesenbauer [a,b,*], Alexander König [a,c], Stefan Gorka [a,b], Lilian Marchand [d], Naoise Nunan [e,f], Barbara Kitzler [g], Erich Inselsbacher [c], Christina Kaiser [a,**]

[a] Division of Terrestrial Ecosystem Research, Centre for Microbiology and Environmental Systems Science, University of Vienna, Vienna, Austria, Djerassiplatz 1, A-1030, Wien, Austria
[b] Doctoral School in Microbiology and Environmental Science, University of Vienna, Vienna, Austria
[c] Institute of Soil Research, University of Natural Resources and Applied Life Sciences – BOKU, Peter-Jordan-Straße 82, 1190, Wien, Austria
[d] Institut Agro Rennes-Angers, France
[e] Sorbonne Université, CNRS, IRD, INRAE, P7, UPEC, Institute of Ecology and Environmental Sciences—Paris, 4 Place Jussieu, 75005, Paris, France
[f] Department of Soil & Environment, Swedish University of Agricultural Sciences, P.O. Box 7014, 75007, Uppsala, Sweden
[g] Department for Forest Ecology and Soil, Austrian Research Centre for Forests, Seckendorff-Gudent-Weg 8, 1131, Vienna, Austria

ARTICLE INFO

Keywords:
Reverse microdialysis
Root exudation
Short-chain fatty acids
Sugar metabolism
Rhizosphere priming effect
Oxygen depletion

ABSTRACT

Root exudation increases the concentration of readily available carbon (C) compounds in its immediate environment. This creates 'hotspots' of microbial activity characterized by accelerated soil organic matter turnover with direct implications for nutrient availability for plants. However, our knowledge of the microbial metabolic processes occurring in the immediate vicinity of roots during and after a root exudation event is still limited.

Using reverse microdialysis, we simulated root exudation by releasing a ^{13}C-labelled mix of low-molecular-weight organic C compounds at mm-sized locations in undisturbed soil. Combined with stable isotope tracing, we investigated the fine-scale temporal and spatial response of microbial metabolism, soil chemistry, and traced microbial respiration and uptake of exuded compounds.

Our results show that a 9-h simulated root exudation pulse leads to i) a large local respiration event and ii) alteration of the temporal dynamics of soil metabolites over the following 12 day at the exudation spot. Notably, we observed a threefold increase in ammonium concentrations at 12 h and increased nitrate concentrations five days after the pulse. Moreover, various short-chain fatty acids (acetate, propionate, formate) increased over the following days, indicating altered microbial metabolic pathways and activity. Phospholipid and neutral lipid fatty acids (PLFAs, NLFAs) of all major microbial groups were significantly ^{13}C-enriched within a 5 mm radius around the microdialysis probes, but not beyond. The highest relative ^{13}C enrichment was observed in fungal NLFAs, indicating that a significant proportion of the exuded compounds had been incorporated into fungal storage compounds.

Our findings indicate that the punctual release of low-molecular-weight organic C compounds into intact soil significantly changes microbial metabolism and activity in its immediate surroundings, enhancing mineralization of native organic nitrogen. This highlights the versatility of microbial metabolic pathways in response to rapidly changing C availability and their effectiveness in increasing nutrient availability near plant roots.

1. Introduction

Roots release a variety of C-rich compounds into their immediate environment (Jones et al., 2009; Canarini et al., 2019). These compounds consist of high-molecular weight compounds such as mucilage and proteins, and low-molecular-weight compounds such as amino acids, organic acids, and sugars (Badri and Vivanco, 2009; Vives-Peris et al., 2020). The latter are predominantly released at the

* Corresponding author. Division of Terrestrial Ecosystem Research, Centre for Microbiology and Environmental Systems Science, University of Vienna, Vienna, Austria, Djerassiplatz 1, A-1030, Wien, Austria.
** Corresponding author.
E-mail addresses: julia.wiesenbauer@univie.ac.at (J. Wiesenbauer), christina.kaiser@univie.ac.at (C. Kaiser).

https://doi.org/10.1016/j.soilbio.2023.109259
Received 18 July 2023; Received in revised form 17 November 2023; Accepted 23 November 2023
Available online 1 December 2023

root tips, either through passive diffusion or active exudation (Badri and Vivanco, 2009; Jones et al., 2009; Canarini et al., 2019). Consequently, due to their constant movement through the soil, tips of growing roots create distinct 'exudation hotspots' of transiently high concentration of low-molecular-weight C compounds (Vogel et al., 2014).

Such pulses of easily available C are thought to stimulate the activity of previously partly starving and thus inactive microbes in the surrounding of the pulse (De Nobili et al., 2001; Mondini et al., 2006; Kuzyakov et al., 2015; Vetterlein et al., 2020). This process is marked by an immediate respiration of the assimilated C (Butler et al., 2004; Kaštovská and Šantrůčková, 2007), followed by an enhanced respiratory activity driven by increased microbial biomass turnover (Blagodatskaya and Kuzyakov, 2008), which is eventually followed by accelerated SOM decomposition - a phenomenon called the rhizosphere priming effect (Kuzyakov, 2002, 2010; Dijkstra et al., 2013; Haichar et al., 2014; Huo et al., 2017). While priming effects are observed in the majority of investigated cases, instances of no or 'negative' priming (i.e. retardation of SOM decomposition) have been reported (Kuzyakov, 2002; Dijkstra et al., 2013; Luo et al., 2016). These findings underscore the complexity of the rhizosphere C-cycling and variability of microbial interactions.

As a result of this accelerated microbial activity, a variety of microbial metabolites is released into the soil solution. Pulses of root exudation and their consequences for microbial activity are referred to as 'hot moments' in soil, implying that these changes in the process rates and metabolite levels last only for a short duration (Kuzyakov et al., 2015). The amount and composition of microbial metabolites released likely reflect the microbial processes occurring in response to the root exudation event but have not been previously measured at the hotspot. Moreover, the actual timeframe of accelerated or altered process rates at hotspots is uncertain and could range from minutes to days (Kuzyakov et al., 2015; Vetterlein et al., 2020). By studying the dynamics of soil metabolites that emerge in response to root exudation, valuable insights can be gained into the metabolic pathways involved in the degradation and transformation of exudate compounds, as well as the timeframe and persistence of the rhizosphere priming effect.

A substantial fraction of the C exuded by roots is incorporated into the rhizosphere microbial biomass (Butler et al., 2004; Denef et al., 2007). It was observed that exudates of young beech trees where preferentially utilized by gram-negative bacteria and fungi (Esperschütz et al., 2009), while gram-positive bacteria appeared to have little reliance on rhizodeposits but perhaps benefitted from later priming effects (Butler et al., 2003; Esperschütz et al., 2009; Balasooriya et al., 2013). Conversely, Cesarz et al. (2013) reported that beech roots did not affect bacterial biomass, but rather led to an increase in the fungi-to-bacteria ratio. This highlights how root exudates may be preferentially utilized by certain microbial groups and shape the microbial community composition (Zhalnina et al., 2018; Seitz et al., 2022), though the specific outcomes remain uncertain.

Researchers have employed various approaches, e.g. rhizoboxes (Wenzel et al., 2001; Chaignon et al., 2002; zu Schweinsberg-Mickan et al., 2010; Spohn et al., 2013) or planar optodes (Santner et al., 2015; Li et al., 2019), to study a range of root and rhizosphere processes, including spatial distribution of microbes, enzymes and chemical compounds. A common drawback of these tool is the limited capacity of time-points, spots, and analytes they can assess, and their struggle with the heterogeneous soil structure. Moreover, such *in situ* studies based on root exudates present their own unique challenges, as the composition and concentration of root exudates cannot be controlled, and the presence of root respiration further complicates the analysis.

Thus, various studies have added powders or solutions containing compounds found in exudates to sieved soil in an attempt to explore e.g. the mechanisms behind rhizosphere priming effects (Basiliko et al., 2012; Nottingham et al., 2012; Koranda et al., 2013; Wild et al., 2014; Girkin et al., 2018; Jilling et al., 2021) or changes in the microbial community (Shi et al., 2011; Mau et al., 2015; Papp et al., 2020). In contrast to root exudation which creates localized high C concentrations with strong concentration gradients (Kuzyakov and Razavi, 2019; Vetterlein et al., 2020), the substrate addition results in uniform distribution of moderately enhanced C availability throughout the whole soil volume, which may affect microbial responses to substrate input considerably. In addition, the intricate mechanisms underlying the rhizosphere priming effect critically depend on the physico-chemical and biotic micro-environment of the root exudation hotspot, which is likely disintegrated by the abovementioned approaches.

Microdialysis allows to release artificial root exudates at small spots into undisturbed soil while at the same time collecting metabolites from the surrounding soil solution. In its classic application, metabolites are collected from the soil solution via a diffusion gradient across a small semi-permeable membrane inserted into the soil (Inselsbacher et al., 2011; Oyewole et al., 2014). By reversing the concentration gradient, i.e. by pumping high levels of low-molecular-weight compounds along the inside of the membrane, compounds can be released via passive diffusion at distinct soil spots (Buckley et al., 2022; König et al., 2022). This way it is possible to create a hotspot of high C concentration, akin to passive root exudation. Compared to Rhizon samplers, which also allow to mimic root exudation by releasing a solution (Kuzyakov et al., 2007; Keiluweit et al., 2015; Baumert et al., 2018), microdialysis has the benefit of not generating a mass flow into the soil by relying exclusively on diffusion. Moreover, the 'reverse' microdialysis approach offers the unique advantage of combining the release of organic compounds with the simultaneous collection of (other) soil metabolites (as by 'classic' microdialysis) at high temporal resolution.

The aim of this study was the detailed analysis of the fine-scale temporal dynamics of microbial activity and soil chemistry in response to a simulated root exudation pulse right at the exudation spot in intact soil. Specifically, we addressed the following questions:

(1) Does a 'root exudation' pulse alter the dynamics of soil metabolites at the exudation hotspot?
(2) What is the timescale and pattern of substrate- and SOM-derived microbial respiration following a simulated root exudation pulse?
(3) Which microbial groups are involved in the metabolism of 'root exudates' in the days following the pulse?

To achieve this, we used reverse microdialysis to release a mixture of ^{13}C-labelled sugars (fructose, glucose) and organic acids (acetate, succinate) into undisturbed soil cores over a period of 9 h while simultaneously collecting metabolites from the soil solution for 12 days. Additionally, we assessed substrate-induced respiration and SOM mineralization, and the uptake of ^{13}C-labelled substrate into different microbial groups. We observed a sequence of microbial processes over time and their limitation in space around the artificial root, marked by long-lasting effects of simulated root exudation on soil biogeochemistry and microbial activity.

2. Material and methods

2.1. Soil sampling

Soil was sampled in a managed mature beech (*Fagus sylvatica*) forest (average tree age around 90 yrs) in Klausen-Leopoldsdorf, Austria (48°07′ N, 16° 03′ E, 510 m asl). The soil is a Dystric Cambisol (over flysch) with a pH of 4.16 ($CaCl_2$) and an organic C and total N content of 5.01% and 0.38%, respectively (Kitzler et al., 2006; Brandstätter et al., 2013; König et al., 2022). We sampled soil on June 6th, 2018 at five locations along a horizontal transect at a distance of 60 cm each. After removing the litter layer, we took triplicate soil cores (10 cm diameter × 6 cm depth) right next to each other from the uppermost soil at each of the five locations. From each triplicate, one soil core was sieved, and the gravimetric soil water content was determined, which ranged between 44 and 53%. Per site, one of the two remaining intact soil cores was used to set up the mesocosms for the experiment (the third soil core served as

a backup).

2.2. Experiment design and microdialysis setup

Paired mesocosms (one for pulse simulation and one for control) were set up for each of the five soil sampling sites by coring two smaller cores (2.8 cm diameter × 3 cm height) from one larger soil core. Intact mesocosm cores were carefully placed in modified polypropylene centrifuge tubes (Greiner Bio-One, 50 ml), which were cut off 4 cm below their screw caps and turned upside-down, so they stood in their closed screw caps (opening screw caps allowed easy collection of the soil at the end of the experiment). One of the two paired mesocosm received a labile substrate pulse (n = 5) while the second mesocosm acted as a control (n = 5), receiving only water.

In order to maximize the soil volume affected by microdialysis within each undisturbed soil core, two microdialysis probes (CMA 20, 20 kDa molecular weight cut-off, 1 cm membrane length, 0.5 mm outer diameter; CMA Microdialysis AB, Kista, Sweeden) were inserted into each mesocosm soil core. To avoid damaging the microdialysis probes, holes were pre-made with steel needles (0.5 mm diameter) to help guide the probes into the soil, which was then gently compressed around it. To ensure that only one sample per hour per mesocosm was collected, the tubes of the two microdialysis probes were joined with a T-connector (Micro T, CMA Microdialysis AB, Kista, Sweden) (Fig. S1). Microdialysis probes were perfused with ultrapure water (Milli-Q) containing low concentrations of KCl (3.848 μM) and MgSO4 (1.595 μM) (from now on called 'background solution') at a perfusion flow rate of 2.5 μl min^{-1} per microdialysis probe using syringe pumps (CMA 4004, CMA Microdialysis AB, Solna, Sweden). The purpose of adding KCl and $MgSO_4$ to the perfusate was to prevent the formation of an osmotic gradient between the perfusate and the soil solution (Demand et al., 2017; Warren, 2018). Samples (dialysates) were collected in refrigerated fraction collectors (CM4 470, CMA Microdialysis AB, Solna, Sweden) and subsequently stored at −20 °C until analysis.

During an initial 3-h period, all microdialysis membranes were perfused with the background solution. This was done to facilitate the formation of water bridges within the soil and to analyse initial concentrations of soil compounds collected in the dialysates. In the following 9 h, we implemented a pulse of labile substrate using reverse microdialysis to mimic root exudation, similar to the diurnal carbon release dynamics observed in natural hotspots with heightened exudation during daylight hours (Murray et al., 2004; Cardon and Gage, 2006). A labile substrate mixture consisting of ^{13}C-labelled acetate, succinate, fructose and glucose (each 125 μmol C l^{-1}, 98 at% ^{13}C, uniformly labelled, Sigma-Aldrich) was added to the background solutions of one mesocosms of each pair (n = 5). These compounds were selected based on their prevalence in natural root exudates of beech trees (Smith, 1976) and to represent a range of chemical structures (sugar, organic acid) commonly found in root exudates (Vives-Peris et al., 2020). We deliberately refrained from including nitrogen-containing compounds, despite acknowledging their significance within root exudate (Drake et al., 2013; Edwards et al., 2018; Chari and Taylor, 2022), in order to focus specifically on the impact of carbon alone - a key element in the root exudate-microbe-soil interaction.

After this pulse, the perfusate was switched back to pure background solution. Control mesocosms received background solution throughout the whole experimental as perfusate. For the first 3 days (72 h), microdialysis was kept running constantly in all mesocosms and dialysates were collected hourly. Subsequently, the pumps were turned off and only switched on for 4 h on day 5, 7, and 12 to collect additional dialysate samples. Throughout the experiment, we monitored the water content by weighing the mesocosms and adjusting it, if necessary, by pipetting Milli-Q onto the surface.

2.3. Microbial responses to simulated root exudation

2.3.1. CO_2 analysis – gas sampling and estimation of respiration rates

Mesocosms were placed in airtight jars fitted with septa for taking gas samples (see Fig. S1). The microdialysis tubing was inserted through the septa to allow simultaneous dialysate collection. We took headspace gas samples at multiple time points during the experiment: on day 1 (hours 2, 6, 7, 8, 9, 10, 13), on days 2 and 3 (twice), and once on days 5, 7 and 12. The $^{12}C–CO_2$ and $^{13}C–CO_2$ concentration of gas samples were measured by a headspace gas sampler (GasBench II, Thermo Fisher Scientific, Bremen, Germany) couple to a isotope ratio mass spectrometry (Delta V Advantage, Thermo Electron, Bremen, Germany). When taking gas samples, the mesocosm jars (105 ml volume) were closed airtight, the first gas sample (15 ml) was taken and the removed air was replaced with artificial air (200 ppm CO_2) to avoid sub-atmospheric pressure. The second gas sample was taken after 60 min incubation time and the mesocosm jars were opened. The CO_2 concentration and ^{13}C signature of the second sample was corrected for the added artificial air. The total respiration rate and its atom percent ^{13}C (at% ^{13}C) signature were calculated from ^{12}C- and $^{13}C–CO_2$ concentration differences between the initial gas sample and the second, corrected, gas sample. The percentage and total amount of respiration originating from the added ^{13}C-labelled substrate and from the native SOM were calculated using a two-pool mixing model with the ^{13}C signature of the added substrate (98 at% ^{13}C) and natural abundance of ^{13}C in the respiration of the control mesocosms (1.08 at% ^{13}C) as end members. For a detailed outline of the calculations see the supplementary materials.

It should be noted that the mesocosms that were to receive the labile substrate pulse exhibited a lower average respiration per gram of mesocosm-soil prior to the substrate pulse and lower SOM-derived respiration persisted throughout the first part of the experiment (Fig. S2). We attribute this to an uneven distribution of stones and organic matter across the mesocosms observed during soil harvest, which we could not control for before the experiment as we did not sieve the soil. To account for this initial variability, we calculated a normalized SOM-derived respiration, in which all respiration measurements were put in relation to the initial respiration (% of initial respiration, Fig. 1). This allows a more accurate comparison of the effect of the labile substrate addition on respiration (Fig. 1). For the original data in nmol CO_2 g^{-1} soil $hour^{-1}$, we refer the reader to Supplementary Fig. S2.

Additionally, we estimated the 'background' SOM-derived respiration in the immediate surrounding of each microdialysis probe, with the assumption that SOM-derived respiration was not locally affected by the substrate input. We calculated the fraction of the SOM-derived respiration obtained per soil core around the microdialysis probe as a cylindrical volume as:

$$R_{background} = R_{SOM} \times DW_{mesocosm} \times \frac{V_{cylinder}}{V_{mesocosm}}$$

where $R_{background}$ is the SOM-derived respiration (nmol CO_2 h^{-1} $V_{cylinder}^{-1}$) within $V_{cylinder}$, the cylindrical soil volume around the microdialysis probe, R_{SOM} is the SOM-derived respiration of the mesocosm (nmol CO_2 h^{-1} g^{-1}), $DW_{mesocosm}$ is the soil dry weight of the mesocosm (g), and $V_{mesocosm}$ is the volume of the mesocosm (mm^3).

We selected a 1-mm radius for our calculations as we aimed to estimate substrate- and SOM-derived respiration over a short 9-h period during which substrate was released. This falls at the lower end of range observed in several studies, which have reported plant root exudates occurring between 0.2 and 2 mm away from the surface of the roots (Falchini et al., 2003; Herman et al., 2006; zu Schweinsberg-Mickan et al., 2010). Occasionally, however, studies have found exudates to disperse up to 5–12 mm (Sauer et al., 2006; Dessureault-Rompré et al., 2007; Finzi et al., 2015).

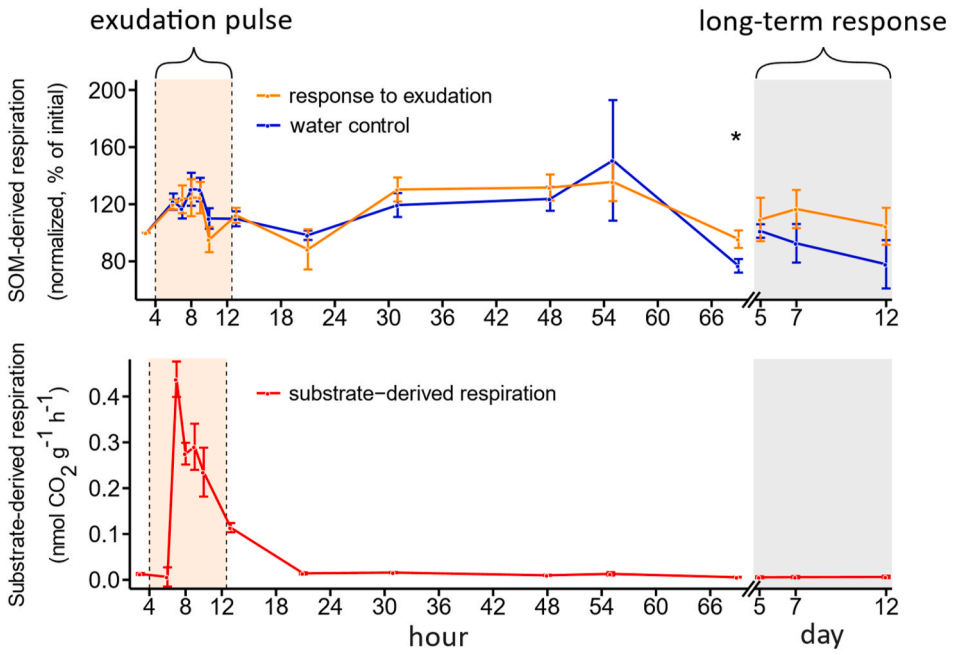

Fig. 1. Temporal dynamics of normalized SOM-derived respiration rate (percentage of initial respiration) and substrate-derived respiration rate. The time of the 9-h long pulse from labile substrate (4–12 h) is highlighted as an orange background and the long-term response (5–12 days) is highlighted as a grey background. The short-term response is depicted in hours and the long-term effects in days and are separated by an x-axis break at hour 72. Top: The normalized SOM-derived respiration rate normalized by dividing by the initial respiration rate in response to the exudation pulse (orange) compared to a water control (blue). Bottom: The respired labile substrate (nmol CO_2 g^{-1} h^{-1}) is shown in red. Depicted are the means and standard error of the mean (n = 5) with asterisks indicating significant differences in response to exudation pulse.

2.3.2. Dialysate analysis (soil chemistry & metabolites)

We measured organic and inorganic anions and sugars in the dialysates using HPLC (Dionex ICS 5000+, Thermo Fisher, Germany). To optimize the chromatographic analyses, we pooled the consecutive hourly dialysates and combined 2, 3 or 4 dialysates for periods 1–20 h, 21–29 h and remaining dialysates, respectively.

Anions were measured on a Dionex IonPac AS11-HC (2 × 250 mm) column with a Dionex IonPac AG11-HC (2 × 50 mm) guard column at a constant flow rate of 0.38 ml min^{-1} with a KOH solvent. We analysed acetate, propionate, formate, butyrate, chloride, nitrate, succinate, malate, sulfate, oxalate, phosphate, and citrate. The HPLC run started at 1 mM KOH (10 min), then increased to 15 mM (1 mM min^{-1}), then to 60 mM (5 mM/min) and kept at this concentration for 5 min and finally the run was ended with 7 min at 1 mM. Sugars (glucose, fructose, galactose, sucrose) were measured on a Thermo CarboPac PA20 (0.4 × 150 mm) column with a Thermo CarboPac PA20G (0.4 × 35 mm) guard column at a constant flow rate of 8 µl min^{-1} with a KOH solvent. We started the run with 10 min of 10 mM KOH, increased to 50 mM for 5 min, increased to 200 mM for 5 min and ended the run with 5 min at 20 mM. The ammonium concentration in dialysates was determined colorimetrically (Kandeler and Gerber, 1988; Hood-Nowotny et al., 2010).

2.3.3. PLFA and NLFA analyses

At the end of the experiment (day 12), we harvested the soil to investigate the ^{13}C enrichment of different microbial groups in soils that received labile ^{13}C-labelled substrate. We harvested soil in the surrounding (<5 mm) and distant (>5 mm, Fig. S3) radius of the microdialysis probes by coring the soil with a rectangular tube (1 cm × 1.5 cm) with the two microdialysis probes in the centre. Afterwards the soil was homogenised by mixing and stones were removed with a tweezer. To determine which microbial groups took up the substrate, we extracted the phospholipid and neutral lipid fatty acids (PLFAs, NLFAs) and used them as biomarkers for different microbial groups and fungal storage, respectively.

Lipids were extracted from lyophilized soils with a mixture of chloroform, methanol, and citrate buffer (v/v/v = 1:2:0.8; (Bligh and Dyer, 1959; Frostegård et al., 1991). Neutral lipids and phospholipids were consecutively eluted on silica solid phase extraction columns with chloroform and methanol, with an acetone washing step in-between. The extracts were subsequently derivatized via mild alkaline methanolysis. The resulting fatty acid methyl esters were analysed on a gas chromatograph (Trace GC Ultra, Thermo Scientific, Germany) coupled to a mass spectrometer (ISQ, Thermo Scientific, Germany) for fatty acid identification and quantification, and on a GC-Ultra (Thermo Fisher Scientific, Milan, Italy) coupled to an isotope ratio MS (Finnigan Delta-V, Thermo Fisher Scientific, Bremen, Germany) via a GC IsoLink (Thermo Fisher Scientific, Bremen, Germany) for determination of isotopic $^{13}C/^{12}C$ ratios. We used nonadecanoic acid methyl ester as an internal standard for quantification, and bacterial and fungal fatty acid methyl esters (BAME CP mix, Supelco; 37 Component FAME mix, Supelco) as qualitative external standards.

Fatty acids of the phospholipid and neutral lipid fractions were assigned to the same phylogenetic groups. Unless otherwise noted, fatty acids were assigned according to (Willers et al., 2015). We assigned the unsaturated fatty acids 14:0, 15:0, 16:0, 17:0 and 18:0 as general microbial markers (data not shown), the mono- and cyclopropyl-unsaturated fatty acids 16:1ω5 (Phillips et al., 2002), 16:1ω7, 17:1ω7, cy17:0 and cy19:0 as markers for gram-negative bacteria, the terminally branched fatty acids i15:0, a15:0, i16:0, i17:0 and a17:0 for gram-positive bacteria (excluding Actinobacteria) (Joergensen and Wichern, 2008), the methyl-branched fatty acids 10Me18:0 and 10Me19:0 for Actinobacteria, and the fatty acids 18:1ω9c, 18:1ω9t and 18:2ω6,9 for fungi. However, we must note that although the 18:1ω9t is reported as specific for fungi (Balser et al., 2005) it can also show patterns similar to gram-negative bacteria biomarkers.

We calculated isotopic enrichment in individual PLFAs and NLFAs as the difference in relative ^{13}C-enrichment of labelled samples to unlabelled control as at% ^{13}C excess (Kaiser et al., 2015). The relative ^{13}C content (µg ^{13}C excess) of individual PLFAs and NLFAs was calculated as relative ^{13}C-enrichment weighted by the mean abundance (in µg C in

FAs g^{-1} dry soil).

2.4. Statistical analysis

All statistical analysis were performed using R (R Core Team, 2022) and all graphs were plotted using ggplot2 (Wickham, 2016). We removed outliers that had values that were higher or lower three times the interquartile range. We tested the normality of the data using Shapiro-Wilk test, and homogeneity of variances using the Levene test.

We tested significant differences of compound concentrations per time point using Mann-Whitney *U* test (Table 1) since the data were neither normal distribution nor showed homogeneity of variances, regardless of data transformation. We log-transformed the respiration data (SOM-derived respiration and normalized SOM-derived respiration) and tested significant differences from control for each time point with Student's two sample *t*-test. The μg C and at% ^{13}C values of PLFA and NLFA biomarker groups were tested for differences between amended mesocosms receiving an exudation pulse compared to the water controls using a Student's two sample *t*-test (Table 2). Moreover, the μg C, μg ^{13}C excess and at% ^{13}C excess of fatty acid biomarker groups were tested for differences between PLFAs and NLFAs using a Student's two sample *t*-test or Mann-Whitney *U* test (Table 3).

3. Results

3.1. Transfer rates and retrieval rates of added labile substrate

The transfer rate of compounds i.e., the percentage of compounds in the perfusate that were actually released into the soil (König et al., 2022), were 31.84% (±0.87 se) for acetate, 15.06% (±1.08) for succinate, 9.15% (±1.21) for glucose and 5.65% (±1.7) for fructose, averaged over the 9-h pulse (Fig. 2: acetate, Fig. S4: succinate, glucose, fructose). This transfer rates correspond to an average 113.43 (±4.89 se) nmol C for acetate, 53.1 (±8.31) nmol C of succinate, 27.92 (±7.41) nmol C of glucose and 18.23 (±5.24) nmol C of fructose, or in sum 212.68 (±22.17) nmol C per mesocosm. The 'retrieval' rates i.e., the percentage of initially exuded compounds, which were retrieved back in the first 2 h after the pulse after switching back to background solution were 6.32% (±0.28 se) for acetate, 16.51% (±4.26) for succinate, 27.67% (±2.99) for glucose and 47.62% (±10.78) for fructose. This retrieval rates correspond to an average 7.14 (±0.33) nmol C acetate, 7.68 (±1.15) nmol C succinate, 9.38 (±0.36) nmol C glucose, and 9.63 (±0.88) nmol C fructose, or in sum 34.53 (±2.30) nmol C per mesocosm. Note that for sugars in particular, the transfer rates dropped to nearly zero percent after 4 h with simultaneously high retrieval rates (Fig. S4), indicating a saturation in sugars around the microdialysis probe after not being removed quickly enough by biological or physical processes.

3.2. Temporal pattern of several soil metabolites is altered after a pulse of labile C compounds over the following 2–12 days

Overall, we found that several soil metabolites, such as acetate, propionate, formate and ammonium, displayed distinct temporal patterns in the hours following the labile substrate pulse, but we also observed longer-term changes in acetate, formate, nitrate and sulfate concentrations several days later (Fig. 2, Table 1). The concentrations of certain small chain organic acids peaked about 24 h after the labile C input (Fig. 2, Table 1). Specifically, acetate concentrations increased significantly 9 h after the end of the input pulse (hour 20) and remained elevated for 34 h (i.e., until hour 53) (Fig. 2, Table 1). Similarly, in the same period, ammonium and propionate concentrations significantly increased compared to the control (hours 26–45 and hours 29–45, respectively). This increase in organic acids and ammonium was accompanied by a significant increase of sulfate during hours 29–33. Following the organic acid peak (acetate, ammonium, propionate) we detected a trend towards higher formate and sulfate concentration. We

Table 1
Statistics on changes in concentrations of compounds collected from soil solution by microdialysis (Fig. 2). Differences in soil metabolite concentration (μM) between soils that received a 9-h labile substrate pulse (n = 5) and a water control (n = 5) were tested by time period (2, 3, or 4 h pooled dialysate). The compounds acetate, succinate, fructose, and glucose were part of the 9-h labile substrate pulse (hour 4–12). The time points for the long-term response are given in days (day 5, 7 and 12). Empty cells indicate that the compound was not detected at the time point. Significant differences ($p < 0.05$) are indicated with asterisks next to an arrow indicating if concentrations were significantly higher (↑*) or lower (↓*) than the water control.

	2	exudation pulse																		day					
hour		4	6	8	10	12	14	16	18	20	23	26	29	33	37	41	45	49	53	57	61	65	69	5	7	12
acetate	–	↑*	↑**	↑**	↑**	↑**	↑**	–	↓*	↑**	↑*	↑*	↑**	↑**	↑*	↑*	↑*	↑*	↑**	↑*	–	↑*	↑*	↑**	↑*	↑*	↑**
succinate	–	↑*	↑*	↑*	↑**	↑**	–			–		–	–	↑*	–	–	–	–	–			–	–	–	–	–
fructose		↑*	↑**	↑*	↑**	↑**	↑*																			
glucose		↑*	↑**	↑*	↑**	↑**	↑*																			
propionate	–	–	–	–	–	–	↓*	↓*	–	–	–	–	↑**	↑**	↑**	↑*	↑*	–	–	–	–	–	–	–	–	–
formate	–	–	↓*	–	–	–	↓**	↓**	↑*	–	–	–	↑**	–	–	–	–	–	–	–	–	–	–	–	–	↑**
ammonium	–	–	–	–	–	–	–	–	↓*	↓*	–	↑**	↑**	–	↑**	↑**	↑*	–	–	–	–	–	–	–	–	–
nitrate	–	–	–	–	–	–	–	–	–	–	–	–	–	–	–	–	–	–	–	–	–	–	–	–	–	↑**
sulfate	–	–	–	–	–	–	–	–	–	–	–	–	↑**	↑*	–	–	↑*	↑*	–	–	–	–	–	–	–	↑*
citrate	–	–	–	–	–	–	–	–	–	–	–					–						–	–	–	–	–
oxalate	–	–	–	–	–	–	–	–	–	–	–	–	–	–	–	↑*	–	–	–	–	–	–	–	–	–	–

Mann-Whitney *U* test, p-value: >0.05 ·, <0.05 *, <0.01 **, <0.001 ***.

Table 2
Response of phospholipid fatty acids (PLFAs) and neutral lipid fatty acids (NLFAs) in the proximity (<5 mm) of the microdialysis probe, 12 days after the simulated root exudation event. The differences of μg C and at% ^{13}C values (PLFA, NLFA) between exudation treatment (n = 5) and water control (n = 5) were tested. Depicted are p-values and asterisks for significant differences ($p < 0.05$).

data	biomarker	fungi			bacteria		
		18:2ω6,9	18:1ω9c	18:1ω9t	gram -	gram +	actino
μg C	PLFA	n.s.	n.s.	n.s.	n.s.	0.015 *	n.s.
	NLFA	n.s.	n.s.	n.s.	n.s.	n.s.	n.s.
at% ^{13}C	PLFA	n.s.	0.009 **	0.018 *	0.029 *	0.005 **	0.019 *
	NLFA	0.004 **	0.010 *	0.015 *	0.040 *	0.010 *	0.019 *

Student's *t*-test, p-value: >0.05 n.s., <0.05 *, <0.01 **, <0.001 ***.

Table 3
Differences between phospholipid fatty acids (PLFAs) and neutral lipid fatty acids (NLFAs) in the proximity (<5 mm) of the microdialysis probe, 12 days after the simulated root exudation event (n = 5). The differences between PLFA and NLFA for μg ^{13}C excess, μg C and at% excess were tested. Depicted are p-values and asterisks for significant differences ($p < 0.05$).

data	fungi			bacteria		
	18:2ω6,9	18:1ω9c	18:1ω9t	gram -	gram +	actino
μg C	n.s.	0.0 ***	0.0 ***	0.0 ***	0.0 ***	0.006 **
μg ^{13}C excess	n.s.	n.s.	0.032 *	n.s.	0.016 *	n.s.
at% ^{13}C excess	n.s.	0.021 *	n.s.	n.s.	n.s.	n.s.

Student's *t*-test (Mann-Whitney *U* test: μg ^{13}C excess), p-value: >0.05 n.s., <0.05 *, <0.01 **, <0.001 ***.

observed a slight increase in nitrate concentrations in the dialysates of all mesocosms over the first three days, but no significant differences between the ones that received an input pulse and the controls.

In the days 5–12, in a longer-term response to the labile substrate input, acetate levels again rose significantly on the third day and remained elevated until day 12. At the end of the experiment, the concentrations of acetate, formate, nitrate and sulfate were significantly higher in the dialysates of the samples that had received the input pulse compared to the control samples (Fig. 2). All other compounds (succinate, oxalate, citrate, glucose, and fructose) were detected in negligible amounts and were not clearly affected by the labile substrate input (Fig. S4). Butyrate, malate, phosphate, chloride, galactose and sucrose were not detected in our samples.

3.3. Rapid microbial respiration of labile substrate during the pulse precedes delayed changes in SOM respiration

Our measurements of ^{13}C concentration in the CO_2 produced during the incubation showed that the added mixture of ^{13}C-labelled C compounds was readily taken up and rapidly respired (Fig. 1). The substrate-derived respiration increased sharply 3 h after the start of the labile substrate pulse and remained elevated for the duration of the 9-h long substrate pulse. Out of the total substrate added, the microbes respired 34%, of which 45% was respired during the initial 2–3 h of the pulse (data published in: König et al., 2022). In the hours following the pulse the substrate-derived respiration levelled off (Fig. 1). In contrast, the SOM-derived respiration was unaffected initially (Fig. 1). On day 3, however, soils that received a labile substrate pulse respired significantly more SOM than the control soils (Welch's *t*-test, $t(6) = -2.52$, $p = 0.045$) when compared in % of their respective initial SOM respiration (Fig. 1). We observed a similar, albeit non-significant, trend of higher normalized SOM-respiration during later time points (day 5, 7, 12).

3.4. Estimated increase in CO_2 respiration at the exudation hotspot

In order to obtain a rough estimate on the magnitude of increase of

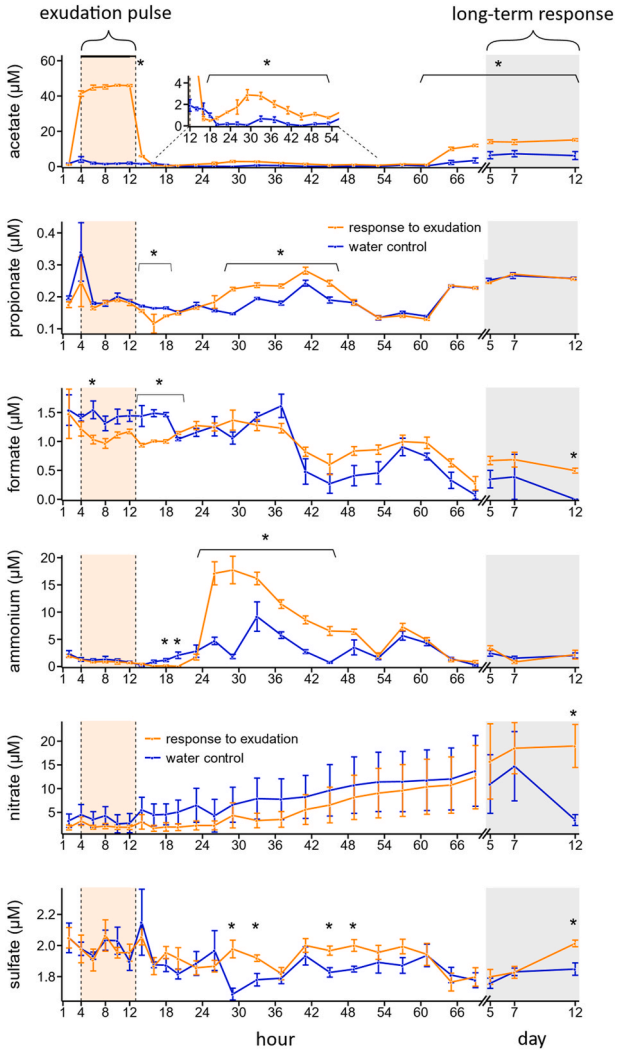

Fig. 2. Temporal dynamics of six soil metabolites (μM; acetate, propionate, formate, ammonium, nitrate, sulfate) in response to a 9-h long substrate pulse (orange) compared to a water control (blue). The time of the exudation pulse (4–12 h) is highlighted as an orange background and the long-term response (5–12 days) is highlighted as a grey background. The short-term response is depicted in hours and the long-term effects in days and are separated by an x-axis break at hour 72. Shown are the mean and standard error of the mean (n = 5) of concentrations in collected dialysate. Acetate was part of the labile substrate pulse and its initial concentration in perfusate is depicted as a black horizontal line. The difference between the black horizontal line and the acetate measurements in dialysates illustrate the net transfer into the soil. Asterisks indicate that the response to labile substrate significantly differs from the water control. Detailed statistics are shown in Table 1. For net transfers and temporal dynamics of succinate, glucose and fructose, as well as temporal dynamics of citrate and oxalate (n.s.) see Fig. S4.

microbial respiration right at the exudation hotspot, we calculated SOM-derived and substrate-derived respiration for a volume within a 1 mm radius around the microdialysis probes, which we assume to be directly affected by the substrate input. We calculated the fraction of the SOM-derived respiration obtained per soil core that occurred in a cylindrical volume of 1 mm radius and 10 mm height, with the aim to estimate the 'background' SOM-derived respiration in the immediate surrounding of each microdialysis probe. We then calculated the cumulative respiration within the hypothetical 1 mm diameter, consisting of the calculated SOM-derived respiration and the measured ^{13}C-substrate-derived respiration (Fig. 3), which we assumed to occur to 100% in the surrounding of the probes (Fig. 4). Based on these assumptions, during the second half of the pulse (hour 7–10), an average additional 10.15 nmol CO_2 (±1.7 se, n = 5) were respired from the added substrate in the immediate surrounding of each microdialysis probe, approximately doubling the respiration within this volume relative to the 'background' SOM-derived respiration (9.36 ± 1.46 se nmol CO_2) (Fig. 3). These calculations rely on our assumption that root exudates would not go beyond a 1 mm radius within 9 h, and that there is no local increase in SOM-derived respiration triggered by the released C compounds. If we would vary the assumed range of root exudates to 0.5, 2 or 5 mm radius within which 2.34, 37.45 and 234.06 nmol CO_2 would be respired from SOM, substrate-derived respiration would increase CO_2 production in this volume by 434, 27 and 4 %, respectively. If there was a local increase in SOM-derived respiration within the chosen radius (which we were unable to measure), we would underestimate the increase in respiration due to the added substrate, as our calculation only includes the substrate-derived respiration plus a volume-based aliquot of the total SOM-derived respiration of the core.

3.5. Phospholipid and neutral lipid fatty acids were ^{13}C enriched in vicinity of the exudation hotspot

All PLFA and NLFA biomarkers, except for the fungi-specific PLFA 18:2ω6,9, were significantly ^{13}C enriched in response to the labile substrate pulse within a 5 mm radius around the microdialysis membranes (at% ^{13}C: Fig. S5, Table 2). There was no significant enrichment in ^{13}C in biomarkers in the soil sampled further away i.e., between 5 and 10 mm around the membranes (Fig. S3). Within the 5 mm radius, the NLFA fungal biomarker 18:1ω9c showed the highest relative ^{13}C enrichment compared to the natural abundance control and was also significantly higher compared to its corresponding PLFA biomarker (at% ^{13}C excess: Fig. 4). The at% ^{13}C excess of the PLFAs and NLFAs from other microbial groups showed no significant differences (Table 3, Fig. 4).

When comparing absolute amounts of μg ^{13}C excess of PLFAs and NLFAs, we found significantly more ^{13}C in PLFA than in NLFA of 18:1ω9t (fungi), gram-positive bacteria, and gram-negative bacteria (not significant), while the fungal marker 18:1ω9c had a tendency (albeit not significant) for higher amounts of ^{13}C excess in NLFAs compared to PLFAs (μg ^{13}C excess: Fig. 4, Table 3). Since we did not find differences in the relative ^{13}C enrichments (at% ^{13}C excess) between PLFAs and NLFAs for 18:1ω9t, gram-negative and gram-positive bacteria, the observed differences in absolute ^{13}C enrichments need to be attributed to the higher absolute amounts (μg C) of PLFAs compared to NLFAs (μg C: Fig. S5).

The labile substrate input significantly increased the microbial biomass (i.e., μg C in PLFAs) of the gram-positive bacteria, but did not affect the biomass of any of the other groups. It also did not affect NLFAs of any microbial group (μg C: Fig. S5). NLFA concentrations were lower compared to PLFA concentrations for all groups except for the fungal biomarker 18:2ω6,9.

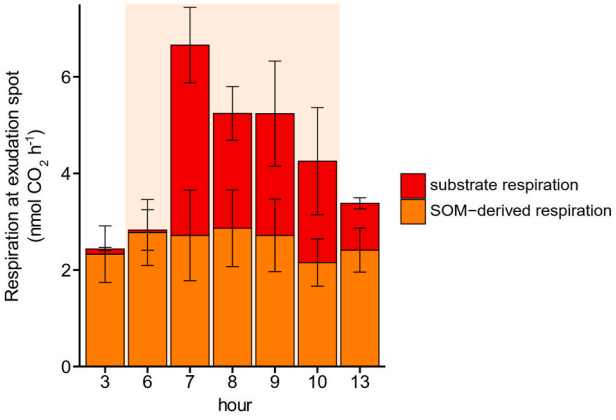

Fig. 3. In this hypothetical calculation, we depict the potential increase in microbial respiration within a 1-mm radius around the microdialysis probes before, during, and after a 9-h long release of readily available C substrates (succinate, acetate, glucose, fructose). The base of the stacked bars represents the aliquot of SOM-derived respiration for a cylindrical soil volume of 10 mm length and 1 mm radius, aiming to represent the immediate surrounding of the microdialysis probes (orange). Note that this calculation assumes that the SOM-derived respiration was homogenously distributed within the core, and not locally affected by the substrate input in the surroundings of the probes. The top of the stacked bars (red) shows the total amount of substrate-derived respiration in each soil core (divided by two), assuming that the released substrate was respired no further than 1 mm from each of the two microdialysis probes per core. Depicted are the means of 5 replicate cores and the standard error of the mean as error bars. The x-axis shows the hours of the experiment with each bar representing a 1-h long respiration measurement. Shaded area indicates the time period in which the substrate was released (4–12 h).

4. Discussion

Our results show that a pulse of organic C compounds released via micro-diffusion at discrete locations in intact soil alters the temporal dynamics of soil metabolites right at these spots over the following hours and days. Interestingly, the concentration of several small-chain fatty acids increased in response to the C input, indicating changes in microbial metabolic pathways. This went along with a strong increase of ammonium availability, indicating microbial mineralization of soil organic N. Our measurements thus support the widely observed phenomenon that labile C compounds exuded by roots lead to enhanced nutrient availability in the rhizosphere (Zhu et al., 2014; Murphy et al., 2015).

4.1. Impact of labile C pulse on microbial activity

Soil microbes respired the released substrate with a 2–3 h delay, which might reflect a physiological lag phase, caused by the need to adapt their internal cellular machinery to the availability of a new substrate (Bertrand, 2019). Had the delayed respiration of the added substrate been due to a slow diffusion of the substrate, we would have seen a steady increase in substrate-derived respiration and no lag phase followed by the very high respiration rates observed (Fig. 1, bottom). It was hypothesized that soil microbes, whose activity is often constrained by C and energy limitations (Blagodatskaya and Kuzyakov, 2013), maintain a state of 'metabolic alertness' to quickly utilize infrequently arriving resources in an otherwise scarce environment (De Nobili et al., 2001; Mondini et al., 2006). The observed 2–3 h delay is consistent with our previous study in which reverse microdialysis was performed with various organic C compounds in different soils (König et al., 2022). There, we observed – after a quick initial transfer – a rapid decline of transfer rates of all compounds into the soil. This indicates (as transfer rates depend on the concentration gradient between the perfusate and the soil), that the released substances accumulated in the soil solution outside the membrane. Transfer rates abruptly increased 3 h later, implying a sudden uptake of the accumulated compounds by microbes after a time delay. These findings, along with the here observed delay in microbial respiration, collectively suggest that microbes in intact soil

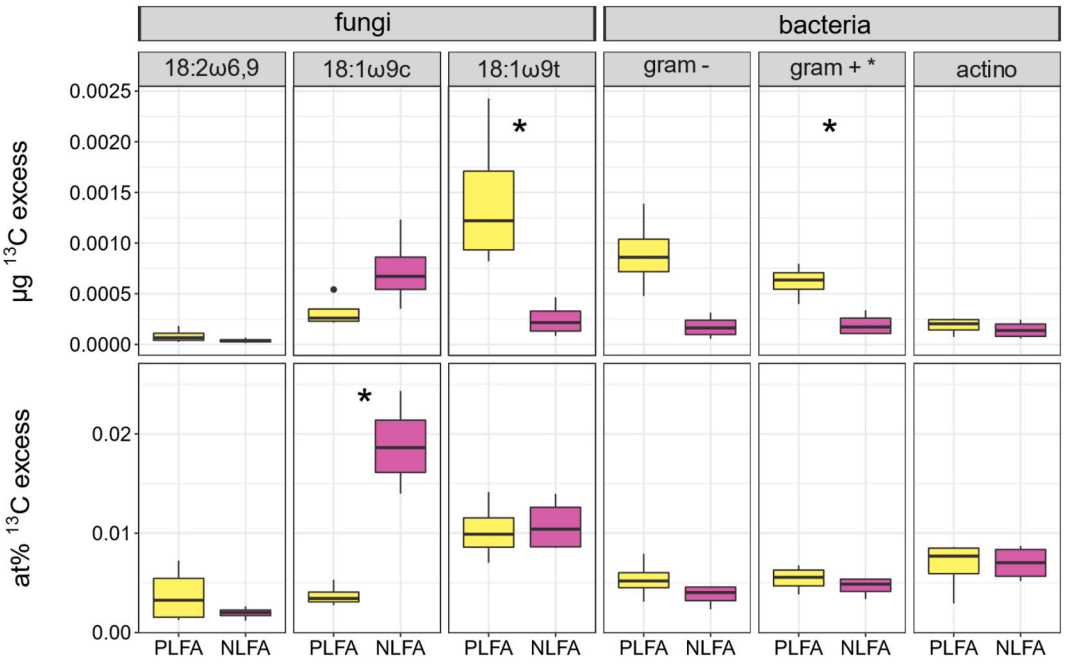

Fig. 4. Enrichment in labile-substrate derived ^{13}C in phospholipid fatty acids (PLFAs, yellow) and neutral lipid fatty acids (NLFAs, pink) in close proximity (<5 mm radius) to the microdialysis probe 12 days after a 9-h pulse of ^{13}C-labelled substrate (n = 5). Due to the significant enrichment observed in all PLFA and NLFA biomarkers (at% ^{13}C: Fig. 3S), except for 18:2ω6,9 PLFA, we have opted to exclusively present the ^{13}C excess data here (µg ^{13}C excess, at% ^{13}C excess). The fungi-specific fatty acid biomarkers 18:1ω9c, 18:1ω9t and 18:2ω6,9 are depicted ungrouped. The remaining fatty acids were grouped into gram-negative bacteria, gram-positive bacteria (*excluding *Actinobacteria*) and *Actinobacteria*. Asterisks indicate significant differences ($p < 0.05$) between PLFA and NLFA for µg ^{13}C excess and at % ^{13}C excess. Detailed statistics are shown in Table 2 and Table 3.

environments undergo a lag phase before taking up and respiring a new substrate.

Organic acids, in contrast to sugars, exhibited higher transfer rates (substrate release) during the pulse and lower back-retrieval rates afterwards, consistent with our previous study in which transfer and retrieval rates were negatively correlated (König et al., 2022). This suggests that sugars accumulated around the membrane after their initial release and were not effectively removed by biotic or abiotic processes like microbial uptake or adsorption to soil surfaces (Jones et al., 2003). Sugars, while widely regarded as ubiquitous substrates that undergo intensive recycling in microbial biomass (Apostel et al., 2015), appeared to be metabolised to a lesser extent by soil microbes compared to organic acids. The relatively quicker removal of organic acids from the membrane surrounding, as indicated by their higher transfer and lower back-retrieval rates, might indicate a more rapid adsorption to soil minerals compared to sugars. However, low-molecular-weight organic substances like glucose and acetate were reported to be consumed within a few hours (Jones et al., 2009), faster than their physico-chemical sorption to the soil (Fischer et al., 2010). To understand the underlying causes for the different behaviour of sugars and organic acids, future experiments should examine each compound class separately. Especially since glucose and acetate may enter different metabolic pathways, such as glycolysis and gluconeogenesis, respectively (Schink et al., 2022).

4.2. Rhizosphere priming effect and nitrogen mineralization

While the strong substrate respiration on the first day did not coincide with an accelerated SOM mineralization, we observed a significant increase in SOM-derived respiration compared to the control starting at day 3 (Fig. 1, top). This 'rhizosphere' priming effect may be attributed to a gradual activation and increase in microbial biomass in response to the added substrate (De Nobili et al., 2001), leading to an increased production of extracellular enzymes that boosted SOM decomposition (Kuzyakov, 2010; Dijkstra et al., 2013). This was further reflected in the up-to-threefold increase in ammonium concentrations within 24 h of substrate input. This indicates N mineralization from SOM and hence accelerated SOM decomposition, which was not yet matched by an increase in SOM-derived respiration (Fig. 1).

Priming effects have been reported to increase N mineralization (Dijkstra et al., 2009; Murphy et al., 2015). Adding C-rich substrate without providing additional N may have induced N-limitation and prompted the microbial community to mine for N (Craine et al., 2007; Fontaine et al., 2011; Brzostek et al., 2013). In a separate microdialysis experiment, sucrose addition was proposed to increase the N demand of the microbial community by alleviating C limitations (Buckley et al., 2022). Consequently, the delayed onset of increased SOM-derived respiration (priming effect) by three days could be partially ascribed to the lack of N in our exudate, which is recognized for its pivotal role in enzyme production (Drake et al., 2013) and, thus, the degradation of SOM. The sequence of events, ranging from substrate respiration to the subsequent increased ammonium concentrations (N-mining) and accelerated SOM-derived respiration (priming effect), can be attributed to the time, energy and N resources required for enzyme production (Liu et al., 2019).

Alternatively, the increase in ammonium concentrations could result from a liberation of previously clay-bound ammonium through organo-mineral interactions with the released organic acids (Keiluweit et al., 2015). We think, however, that this is an unlikely explanation, as the steep ammonium peak occurred only 24 h after the release of organic acids, at a time when both acetate and succinate were only present at much smaller than initial (acetate) or even negligible (succinate) concentrations (Fig. 2). From day 5 onwards, the increased nitrate concentration compared to the controls indicates microbial nitrification, probably triggered by the high amounts of ammonium. Besides nitrate, the elevated levels of acetate (days 3–12), formate (day 12), and sulfate (day 12; Fig. 2, Table 1), imply long lasting changes in soils that received labile substrate.

It should be noted that our experimental design placed limitations on the measurement sensitivity of a spatially constrained priming event.

Specifically, the high background of SOM-derived respiration of the whole soil core may have masked the local increase of SOM-derived respiration within the small volume influenced around the two microdialysis membranes. However, this 294:1 vol ratio (assuming a 1 mm radius of influenced soil around the two membranes) implies that the actual priming effect at the exudation hotspot on the third day was likely considerably higher than our observation suggests.

4.3. Altered metabolic pathways in response to labile C

Simultaneous with the onset of the 24-h long ammonium peak, other organic and inorganic compounds increased: acetate concentrations increased 6 h prior, while propionate, sulfate, and formate concentrations increased 3, 3 and 15 h after the onset of the ammonium peak (Fig. 2), suggesting a complex interplay of metabolic pathways. The organic acids could be fermentation products, indicating potential anaerobic conditions. However, in high glucose environments, it has been shown that *E. coli* cultures favour fermentation over respiration, leading to the release of high concentrations of acetate, even when oxygen is available (Luli and Strohl, 1990; Chacón et al., 2018; Mori et al., 2019). Remarkably, many bacteria employ these respiro-fermentative overflow metabolism and still attain high growth rates (Wortel et al., 2018). For thermo-dynamical reasons, heterotrophic microbes face a trade-off between growth rate and yield (Pfeiffer et al., 2001; Kreft and Bonhoeffer, 2005), which becomes particularly relevant under conditions of abundant resource or limited oxygen supply. Under such conditions the ATP production rate of respiration saturates rapidly and microbes can maximize growth rate at the expense of yield by switching at least partly to incomplete metabolic pathways. In *E. coli*, the growth-rate dependent acetate overflow was explained by fermentation being favoured at high growth rates due to its lower biosynthesis cost relative to the electron transport chain (Basan et al., 2015). Alternatively, the membrane real estate hypothesis proposes that at high growth rates, cells increase in size, reducing their available membrane area for respiratory proteins, prompting a shift towards less efficient but faster ATP production through fermentation (Szenk et al., 2017). Additionally, it was suggested that under nutrient limitations excess C may be routed to overflow respiration or excreted, to accommodate the decomposers stoichiometric requirements (Schimel and Weintraub, 2003; Manzoni and Porporato, 2009).

Interestingly, this would also be a viable strategy for microbes under aerobe conditions, given that microbes face a surplus of sugars (Lipson, 2015). Incomplete metabolic pathways, such as fermentation, allow a higher substrate flux per unit of time but go along with the release of metabolic intermediates such as acetate (Pfeiffer and Bonhoeffer, 2003). The release of high glucose levels at local exudation hotspots could thus have created the right conditions for this glucose-mediated aerobe acidogenesis to take place. Moreover, nutrient limitations induced by the absence of N in the exudate could have resulted in the redirection of surplus C towards excretion or potentially overflow respiration to meet the decomposers stoichiometric requirements (Schimel and Weintraub, 2003; Manzoni and Porporato, 2009). The reduction in the organic acid peaks, e.g., acetate starting at hour 33, signifies a transition from a period of rapid growth with organic acid production to a slower growth phase involving the assimilation of the excreted organic acids. This switch is likely driven by the depletion of the organic acid-producing carbon sources (e.g., sugars) (Wolfe, 2005). Collectively, our findings suggest altered metabolic pathways and microbial activity in the days following the substrate input. Going forward, it should be taken into account that high concentrations of organic acids, like acetate and formate measured in the rhizosphere solution of beach trees (*Fagus sylvatica*) (Fender et al., 2013), might originate from microbial excretion just as likely as from root exudates, highlighting the need for careful interpretation in future studies.

4.4. Oxygen depletion at the exudation hotspot

It is, however, also possible that microbial respiration in the immediate vicinity of the exudation spot caused a temporary depletion of oxygen (O_2) at the spot due to the additional respiration of the released substances: If we assume a pore space of approx. 50% of the soil volume (Voltolini et al., 2017), the 1 mm cylinder around each microdialysis probe will contain a pore volume of 15.71 mm^3. We calculated that, based on oxygen saturation levels of 9.1 mg l^{-1} (20 °C) in water and a concentration of 20.95% O_2 in (atmospheric) air the total amount of available O_2 within such a cylinder would be around 75.7 nmol O_2 (assuming a 50% water saturation of the soil pores), with only 2.24 nmol O_2 being dissolved and thus immediately available in water-filled soil pores (Supplementary material). Comparing this potential O_2 availability with the estimated increased O_2 demand for respiration (SOM-derived plus substrate-derived) of around 19.52 nmol CO_2 (nmol O_2, hour 7–10) during the 9-h long labile substrate pulse (Fig. 3) suggests that a temporary depletion of O_2 concentrations in the vicinity of the substrate input is possible. While it is unknown whether the release of high concentrations of organic compounds leads to temporary oxygen depletion around roots, the formation of anoxic hotspots has been shown in an artificial pore system caused by increased bacterial oxygen consumption at locations with high C availability (Borer et al., 2018). If temporary oxygen depletion occurs around root exudation hotspots it would have consequences for microbial metabolism. Microbes could, for instance, switch to an anaerobic metabolism, which would also go along with shorter, incomplete catabolic pathways that lead to a release of intermediates, such as acetate (Kreft et al., 2020). Moreover, when oxygen concentrations are low, nitrate can serve as an alternative electron acceptor, to allow the oxidation of SOM to CO_2 (Nannipieri and Eldor, 2009; Song et al., 2023). In this case, nitrate is reduced to ammonium in a process called dissimilatory nitrate reduction (Takaya, 2002; Nannipieri and Eldor, 2009), which might also have contributed, to the increased ammonium concentrations we observed at around hour 26–45.

4.5. Substrate utilization by microbial groups and fungal strategies

All microbial groups were significantly ^{13}C enriched exclusively within a 5 mm radius of the exudation pulse (at% ^{13}C: Fig. S5, Table 2). This suggests that the volume of influence of the exudation pulse, and thus the uptake of the ^{13}C-labelled substrate, was limited to the immediate vicinity of the input. This is consistent with the observations that most methods find the rhizosphere to extend between 0.5 and 4 mm (Kuzyakov and Razavi, 2019). Notably, among the microbial groups investigated, only the biomass of gram-positive bacteria significantly increased in response to the labile substrate pulse (µg C: Fig. 4S and Table 2). This was surprising, as we would instead have expected a biomass increase in gram-negative bacteria biomass, which are believed to primarily rely on simple (plant-derived) C compounds (Butler et al., 2003; Kramer and Gleixner, 2008). For instance, in the rhizosphere of young beech trees exudates were preferentially utilized by gram-negative bacteria and fungi, with gram-positive bacteria exhibiting little reliance on rhizodeposits (Esperschütz et al., 2009). Gram-positive bacteria, thought to prefer more complex C forms, were proposed to utilize older soil organic carbon upon fresh root exudate inputs (Bird et al., 2011). Consequently, the increase in gram-positive biomass seen 12 days after the labile substrate pulse may be attributed to them benefitting from priming SOM degradation.

PLFAs and NLFAs of the microbial groups (except 18:1ω9c) did not differ in their relative ^{13}C enrichment (at% ^{13}C excess: Fig. 4, Table 3). Still, gram-negative bacteria and gram-positive bacteria incorporated more ^{13}C into PLFAs than NLFAs in absolute amounts (µg ^{13}C excess: Fig. 4) which can be attributed to their higher concentrations of PLFAs compared to NLFAs (µg C: Fig. S5). Given that the extraction of fatty acids occurred 12 days after the substrate pulse, the ^{13}C incorporation

does not discern groups that initially utilized ^{13}C; rather, it identifies microbial groups that benefitted directly (initial uptake) or indirectly (cross-feeding) from the added substrate over the experimental duration.

Interestingly, we found that the three fungal fatty acid biomarkers responded very differently to the labile substrate input. The fungi-specific biomarker 18:1ω9c exhibited significantly higher at% ^{13}C excess in NLFAs than PLFAs (Fig. 4). In contrast, the 18:1ω9t fungal biomarker did not differ in relative ^{13}C enrichment between PLFAs and NLFAs (Fig. 4, bottom), but had higher absolute amounts of ^{13}C (μg ^{13}C excess) in PLFAs (Fig. 4, top). The fungal biomarker 18:2ω6,9 was the least responsive to the labile substrate input, with overall low fatty acid biomass, no significant enrichment of ^{13}C in the PLFAs, and only little ^{13}C incorporated into NLFAs (Fig. 4, Fig. S5). Under the assumption that these fatty acids are representative for different fungal groups or species (Joergensen, 2022), our data may reflect different fungal strategies. While PLFA are part of cell membranes, NLFA originate form fungal storage compounds (Bååth, 2003). Some fungi (represented by 18:1ω9c) may thus have invested into storage compounds whereas others (represented by 18:1ω9t) could have invested into biomass growth (PLFA). Alternatively, it could also be that fungi use the 18:1ω9c NLFA as a storage compound and incorporate the 18:1ω9t PLFA into cell membranes.

5. Conclusion

Our experiment demonstrated the complex microbial response to a spatially constrained input of labile C compounds, i.e. simulating root exudation, in an undisturbed soil. Our findings suggest that such an input pulse has altered microbial metabolism and increased nutrient availability around the exudation spot, revealing the time frame in which this might occur. We were able to identify a three-stage microbial response to artificial root exudation: First, a rapid local substrate respiration (2–3 h), likely depleting oxygen at the exudation spot; secondly, the initiation of (anaerobic) metabolic pathways, accompanied by the production of fermentation byproducts like organic acids and the release of N-compounds (ammonium) (onset approx. 24 h); and thirdly, the accelerated respiration of organic matter (day 3). Regardless, there are several aspects of root exudation we could not capture with our experimental design, such as the release of a more complex mixture of chemical compounds (including N and P), or the presence of an already specialised rhizosphere community inhabiting the root's surface. Our results provide valuable insights into the potential cascade of effects following a substrate pulse, thereby advancing our understanding of the underlying mechanisms of rhizosphere priming.

CRediT authorship contribution statement

Julia Wiesenbauer: Formal analysis, Investigation, Methodology, Software, Validation, Visualization, Writing – original draft, Writing – review & editing. **Alexander König:** Investigation, Methodology, Software, Visualization. **Stefan Gorka:** Formal analysis, Investigation, Methodology, Software, Validation, Writing – original draft, Writing – review & editing. **Lilian Marchand:** Investigation, Methodology. **Naoise Nunan:** Writing – review & editing, Funding acquisition. **Barbara Kitzler:** Resources. **Erich Inselsbacher:** Methodology, Resources, Writing – review & editing, Funding acquisition. **Christina Kaiser:** Conceptualization, Funding acquisition, Methodology, Project administration, Resources, Supervision, Validation, Writing – review & editing, Writing – original draft.

Declaration of competing interest

The authors declare that they have no known competing financial interests or personal relationships that could have appeared to influence the work reported in this paper.

Data availability

Data to this article can be found online at https://doi.org/10.5281/zenodo.8109601.

Acknowledgements

This study was funded by the Austrian Science Fund (FWF, project P30339–B29) and the European Research Council (ERC) under the European Union's Horizon 2020 research and innovation programme (grant agreement No 819446). We thank Dagmar Woebken, Andreas Richter and Hannes Schmidt for valuable discussions on the experimental design and interpretation of the results, Ludwig Seidl and Margarete Watzka for technical support.

Appendix A. Supplementary data

Supplementary data to this article can be found online at https://doi.org/10.1016/j.soilbio.2023.109259.

References

Apostel, C., Dippold, M., Kuzyakov, Y., 2015. Biochemistry of hexose and pentose transformations in soil analyzed by position-specific labeling and 13C-PLFA. Soil Biology and Biochemistry 80, 199–208. https://doi.org/10.1016/j.soilbio.2014.09.005.

Bååth, E., 2003. The use of neutral lipid fatty acids to indicate the physiological conditions of soil fungi. Microbial Ecology 45, 373–383. https://doi.org/10.1007/s00248-003-2002-y.

Badri, D.V., Vivanco, J.M., 2009. Regulation and function of root exudates. Plant, Cell and Environment 32, 666–681. https://doi.org/10.1111/j.1365-3040.2009.01926.x.

Balasooriya, W.K., Huygens, D., Denef, K., Roobroeck, D., Verhoest, N.E.C., Boeckx, P., 2013. Temporal variation of rhizodeposit-C assimilating microbial communities in a natural wetland. Biology and Fertility of Soils 49, 333–341. https://doi.org/10.1007/s00374-012-0729-7.

Balser, T.C., Treseder, K.K., Ekenler, M., 2005. Using lipid analysis and hyphal length to quantify AM and saprotrophic fungal abundance along a soil chronosequence. Soil Biology and Biochemistry 37, 601–604. https://doi.org/10.1016/j.soilbio.2004.08.019.

Basan, M., Hui, S., Okano, H., Zhang, Z., Shen, Y., Williamson, J.R., Hwa, T., 2015. Overflow metabolism in Escherichia coli results from efficient proteome allocation. Nature 528, 99–104. https://doi.org/10.1038/nature15765.

Basiliko, N., Stewart, H., Roulet, N.T., Moore, T.R., 2012. Do root exudates enhance peat decomposition? Geomicrobiology Journal 29, 374–378. https://doi.org/10.1080/01490451.2011.568272.

Baumert, V.L., Vasilyeva, N.A., Vladimirov, A.A., Meier, I.C., Kögel-Knabner, I., Mueller, C.W., 2018. Root exudates induce soil macroaggregation facilitated by fungi in subsoil. Frontiers in Environmental Science 6. https://doi.org/10.3389/fenvs.2018.00140.

Bertrand, R.L., 2019. Lag Phase Is a Dynamic, Organized, Adaptive, and Evolvable Period that Prepares Bacteria for Cell Division.

Bird, J.A., Herman, D.J., Firestone, M.K., 2011. Rhizosphere priming of soil organic matter by bacterial groups in a grassland soil. Soil Biology and Biochemistry 43, 718–725. https://doi.org/10.1016/j.soilbio.2010.08.010.

Blagodatskaya, E., Kuzyakov, Y., 2008. Mechanisms of real and apparent priming effects and their dependence on soil microbial biomass and community structure: critical review. Biology and Fertility of Soils 45, 115–131. https://doi.org/10.1007/s00374-008-0334-y.

Blagodatskaya, E., Kuzyakov, Y., 2013. Soil Biology & Biochemistry Active microorganisms in soil : critical review of estimation criteria and approaches. Soil Biology and Biochemistry 67, 192–211. https://doi.org/10.1016/j.soilbio.2013.08.024.

Bligh, E.G., Dyer, W.J., 1959. A rapid method of total lipid extraction and purification. Canadian Journal of Philosophy 37, 911–917.

Borer, B., Tecon, R., Or, D., 2018. Spatial organization of bacterial populations in response to oxygen and carbon counter-gradients in pore networks. Nature Communications 9, 769. https://doi.org/10.1038/s41467-018-03187-y.

Brandstätter, C., Keiblinger, K., Wanek, W., Zechmeister-Boltenstern, S., 2013. A closeup study of early beech litter decomposition: potential drivers and microbial interactions on a changing substrate. Plant and Soil 371, 139–154. https://doi.org/10.1007/s11104-013-1671-7.

Brzostek, E.R., Greco, A., Drake, J.E., Finzi, A.C., 2013. Root carbon inputs to the rhizosphere stimulate extracellular enzyme activity and increase nitrogen availability in temperate forest soils. Biogeochemistry 115, 65–76. https://doi.org/10.1007/s10533-012-9818-9.

Buckley, S., Brackin, R., Näsholm, T., Schmidt, S., Jämtgård, S., 2022. The influence of sucrose on soil nitrogen availability – a root exudate simulation using microdialysis. Geoderma 409. https://doi.org/10.1016/j.geoderma.2021.115645.

Butler, J.L., Bottomley, P.J., Griffith, S.M., Myrold, D.D., 2004. Distribution and turnover of recently fixed photosynthate in ryegrass rhizospheres. Soil Biology and Biochemistry 36, 371–382. https://doi.org/10.1016/j.soilbio.2003.10.011.

Butler, J.L., Williams, M.A., Bottomley, P.J., Myrold, D.D., 2003. Microbial community dynamics associated with rhizosphere carbon flow. Applied and Environmental Microbiology 69, 6793–6800. https://doi.org/10.1128/AEM.69.11.6793-6800.2003.

Canarini, A., Kaiser, C., Merchant, A., Richter, A., Wanek, W., 2019. Root exudation of primary metabolites: mechanisms and their roles in plant responses to environmental stimuli. Frontiers in Plant Science 10. https://doi.org/10.3389/fpls.2019.00157.

Cardon, Z.G., Gage, D.J., 2006. Resource exchange in the rhizosphere: molecular tools and the microbial perspective. Annual Review of Ecology, Evolution, and Systematics 37, 459–488. https://doi.org/10.1146/annurev.ecolsys.37.091305.110207.

Cesarz, S., Fender, A.-C., Beyer, F., Valtanen, K., Pfeiffer, B., Gansert, D., Hertel, D., Polle, A., Daniel, R., Leuschner, C., Scheu, S., 2013. Roots from beech (Fagus sylvatica L.) and ash (Fraxinus excelsior L.) differentially affect soil microorganisms and carbon dynamics. Soil Biology and Biochemistry 61, 23–32. https://doi.org/10.1016/j.soilbio.2013.02.003.

Chacón, J.M., Möbius, W., Harcombe, W.R., 2018. The spatial and metabolic basis of colony size variation. ISME Journal 12, 669–680. https://doi.org/10.1038/s41396-017-0038-0.

Chaignon, V., Di Malta, D., Hinsinger, P., 2002. Fe-deficiency increases Cu acquisition by wheat cropped in a Cu-contaminated vineyard soil. New Phytologist 154, 121–130. https://doi.org/10.1046/j.1469-8137.2002.00349.x.

Chari, N.R., Taylor, B.N., 2022. Soil organic matter formation and loss are mediated by root exudates in a temperate forest. Nature Geoscience 15, 1011–1016. https://doi.org/10.1038/s41561-022-01079-x.

Craine, J.M., Morrow, C., Fierer, N., 2007. Microbial NITROGEN LIMITATION INCREASES DECOMPOSITION. Ecology 88, 2105–2113. https://doi.org/10.1890/06-1847.1.

De Nobili, M., Contin, M., Mondini, C., Brookes, P.C., 2001. Soil microbial biomass is triggered into activity by trace amounts of substrate. Soil Biology and Biochemistry 33, 1163–1170. https://doi.org/10.1016/S0038-0717(01)00020-7.

Demand, D., Schack-Kirchner, H., Lang, F., 2017. Assessment of diffusive phosphate supply in soils by microdialysis. Zeitschrift Fur Pflanzenernahrung Und Bodenkunde 180, 220–230. https://doi.org/10.1002/jpln.201600412.

Denef, K., Bubenheim, H., Lenhart, K., Vermeulen, J., Cleemput, O.V., Boeckx, P., 2007. Community Shifts and Carbon Translocation within Metabolically-Active Rhizosphere Microorganisms in Grasslands under Elevated CO2.

Dessureault-Rompré, J., Nowack, B., Schulin, R., Luster, J., 2007. Spatial and temporal variation in organic acid anion exudation and nutrient anion uptake in the rhizosphere of Lupinus albus L. Plant and Soil 301, 123–134. https://doi.org/10.1007/s11104-007-9427-x.

Dijkstra, F.A., Bader, N.E., Johnson, D.W., Cheng, W., 2009. Does accelerated soil organic matter decomposition in the presence of plants increase plant N availability? Soil Biology and Biochemistry 41, 1080–1087. https://doi.org/10.1016/j.soilbio.2009.02.013.

Dijkstra, F.A., Carrillo, Y., Pendall, E., Morgan, J.A., 2013. Rhizosphere priming: a nutrient perspective. Frontiers in Microbiology 4. https://doi.org/10.3389/fmicb.2013.00216.

Drake, J.E., Darby, B.A., Giasson, M.A., Kramer, M.A., Phillips, R.P., Finzi, A.C., 2013. Stoichiometry constrains microbial response to root exudation-insights from a model and a field experiment in a temperate forest. Biogeosciences 10, 821–838. https://doi.org/10.5194/bg-10-821-2013.

Edwards, K.R., Kaštovská, E., Borovec, J., Šantrůčková, H., Picek, T., 2018. Species effects and seasonal trends on plant efflux quantity and quality in a spruce swamp forest. Plant and Soil 426, 179–196. https://doi.org/10.1007/s11104-018-3610-0.

Esperschütz, J., Buegger, F., Winkler, J.B., Munch, J.C., Schloter, M., Gattinger, A., 2009. Microbial response to exudates in the rhizosphere of young beech trees (Fagus sylvatica L.) after dormancy. Soil Biology and Biochemistry 41, 1976–1985. https://doi.org/10.1016/j.soilbio.2009.07.002.

Falchini, L., Naumova, N., Kuikman, P.J., Bloem, J., Nannipieri, P., 2003. CO2 evolution and denaturing gradient gel electrophoresis profiles of bacterial communities in soil following addition of low molecular weight substrates to simulate root exudation. Soil Biology and Biochemistry 35, 775–782. https://doi.org/10.1016/S0038-0717(03)00105-6.

Fender, A.-C., Gansert, D., Jungkunst, H.F., Fiedler, S., Beyer, F., Schützenmeister, K., Thiele, B., Valtanen, K., Polle, A., Leuschner, C., 2013. Root-induced tree species effects on the source/sink strength for greenhouse gases (CH4, N2O and CO2) of a temperate deciduous forest soil. Soil Biology and Biochemistry 57, 587–597. https://doi.org/10.1016/j.soilbio.2012.08.004.

Finzi, A.C., Abramoff, R.Z., Spiller, K.S., Brzostek, E.R., Darby, B.A., Kramer, M.A., Phillips, R.P., 2015. Rhizosphere processes are quantitatively important components of terrestrial carbon and nutrient cycles. Global Change Biology 21, 2082–2094. https://doi.org/10.1111/gcb.12816.

Fischer, H., Ingwersen, J., Kuzyakov, Y., 2010. Microbial uptake of low-molecular-weight organic substances out-competes sorption in soil. European Journal of Soil Science 61, 504–513. https://doi.org/10.1111/j.1365-2389.2010.01244.x.

Fontaine, S., Henault, C., Aamor, A., Bdioui, N., Bloor, J.M.G., Maire, V., Mary, B., Revaillot, S., Maron, P.A., 2011. Fungi mediate long term sequestration of carbon and nitrogen in soil through their priming effect. Soil Biology and Biochemistry 43, 86–96. https://doi.org/10.1016/j.soilbio.2010.09.017.

Frostegård, Å., Tunlid, A., Bååth, E., 1991. Microbial biomass measured as total lipid phosphate in soils of different organic content. Journal of Microbiological Methods 14, 151–163. https://doi.org/10.1016/0167-7012(91)90018-L.

Girkin, N.T., Turner, B.L., Ostle, N., Craigon, J., Sjögersten, S., 2018. Root exudate analogues accelerate CO2 and CH4 production in tropical peat. Soil Biology and Biochemistry 117, 48–55. https://doi.org/10.1016/j.soilbio.2017.11.008.

Haichar, F. el Z., Santaella, C., Heulin, T., Achouak, W., 2014. Root exudates mediated interactions belowground. Soil Biology and Biochemistry 77, 69–80. https://doi.org/10.1016/j.soilbio.2014.06.017.

Herman, D.J., Johnson, K.K., Jaeger, C.H., Schwartz, E., Firestone, M.K., 2006. Root influence on nitrogen mineralization and nitrification in avena barbata rhizosphere soil. Soil Science Society of America Journal 70, 1504–1511. https://doi.org/10.2136/sssaj2005.0113.

Hood-Nowotny, R., Umana, N.H.-N., Inselbacher, E., Oswald- Lachouani, P., Wanek, W., 2010. Alternative methods for measuring inorganic, organic, and total dissolved nitrogen in soil. Soil Science Society of America Journal 74, 1018–1027. https://doi.org/10.2136/sssaj2009.0389.

Huo, C., Luo, Y., Cheng, W., 2017. Rhizosphere priming effect: a meta-analysis. Soil Biology and Biochemistry 111, 78–84. https://doi.org/10.1016/j.soilbio.2017.04.003.

Inselsbacher, E., Öhlund, J., Jämtgård, S., Huss-Danell, K., Näsholm, T., 2011. The potential of microdialysis to monitor organic and inorganic nitrogen compounds in soil. Soil Biology and Biochemistry 43, 1321–1332. https://doi.org/10.1016/j.soilbio.2011.03.003.

Jilling, A., Keiluweit, M., Gutknecht, J.L.M., Grandy, A.S., 2021. Priming mechanisms providing plants and microbes access to mineral-associated organic matter. Soil Biology and Biochemistry 158, 108265. https://doi.org/10.1016/j.soilbio.2021.108265.

Joergensen, R.G., 2022. Phospholipid fatty acids in soil—drawbacks and future prospects. Biology and Fertility of Soils 58, 1–6. https://doi.org/10.1007/s00374-021-01613-w.

Joergensen, R.G., Wichern, F., 2008. Quantitative assessment of the fungal contribution to microbial tissue in soil. Soil Biology and Biochemistry 40, 2977–2991. https://doi.org/10.1016/j.soilbio.2008.08.017.

Jones, D.L., Dennis, P.G., Owen, A.G., Van Hees, P.A.W., 2003. Organic acid behavior in soils - misconceptions and knowledge gaps. Journal of Intelligent and Robotic Systems: Theory and Applications 248, 31–41. https://doi.org/10.1023/A.

Jones, D.L., Nguyen, C., Finlay, R.D., 2009. Carbon flow in the rhizosphere: carbon trading at the soil-root interface. Plant and Soil 321, 5–33. https://doi.org/10.1007/s11104-009-9925-0.

Kaiser, C., Kilburn, M.R., Clode, P.L., Fuchslueger, L., Koranda, M., Cliff, J.B., Solaiman, Z.M., Murphy, D.V., 2015. Exploring the transfer of recent plant photosynthates to soil microbes: mycorrhizal pathway vs direct root exudation. New Phytologist 205, 1537–1551. https://doi.org/10.1111/nph.13138.

Kandeler, E., Gerber, H., 1988. Short-term assay of soil urease activity using colorimetric determination of ammonium. Biology and Fertility of Soils 6, 68–72. https://doi.org/10.1007/BF00257924.

Kaštovská, E., Šantrůčková, H., 2007. Fate and dynamics of recently fixed C in pasture plant–soil system under field conditions. Plant and Soil 300, 61–69. https://doi.org/10.1007/s11104-007-9388-0.

Keiluweit, M., Bougoure, J.J., Nico, P.S., Pett-Ridge, J., Weber, P.K., Kleber, M., 2015. Mineral protection of soil carbon counteracted by root exudates. Nature Climate Change 5, 588–595.

Kitzler, B., Zechmeister-Boltenstern, S., Holtermann, C., Skiba, U., Butterbach-Bahl, K., 2006. Nitrogen oxides emission from two beech forests subjected to different nitrogen loads. Biogeosciences 3, 293–310. https://doi.org/10.5194/bg-3-293-2006.

König, A., Wiesenbauer, J., Gorka, S., Marchand, L., Kitzler, B., Inselsbacher, E., Kaiser, C., 2022. Reverse microdialysis: a window into root exudation hotspots. Soil Biology and Biochemistry 174, 108829. https://doi.org/10.1016/j.soilbio.2022.108829.

Koranda, M., Kaiser, C., Fuchslueger, L., Kitzler, B., Sessitsch, A., Zechmeister-Boltenstern, S., Richter, A., 2013. Seasonal variation in functional properties of microbial communities in beech forest soil. Soil Biology and Biochemistry 60, 95–104. https://doi.org/10.1016/j.soilbio.2013.01.025.

Kramer, C., Gleixner, G., 2008. Soil organic matter in soil depth profiles: distinct carbon preferences of microbial groups during carbon transformation. Soil Biology and Biochemistry 40, 425–433. https://doi.org/10.1016/j.soilbio.2007.09.016.

Kreft, J.-U., Bonhoeffer, S., 2005. The evolution of groups of cooperating bacteria and the growth rate versus yield trade-off. Microbiology 151, 637–641. https://doi.org/10.1099/mic.0.27415-0.

Kreft, J.U., Griffin, B.M., González-Cabaleiro, R., 2020. Evolutionary causes and consequences of metabolic division of labour: why anaerobes do and aerobes don't. Current Opinion in Biotechnology 62, 80–87. https://doi.org/10.1016/j.copbio.2019.08.008.

Kuzyakov, Y., 2010. Priming effects: interactions between living and dead organic matter. Soil Biology and Biochemistry 42, 1363–1371. https://doi.org/10.1016/j.soilbio.2010.04.003.

Kuzyakov, Y., 2002. Review : factors affecting rhizosphere priming effects. Journal of Plant Nutrition and Soil Science 165, 382–396.

Kuzyakov, Y., Blagodatskaya, E., Blagodatskaya, E., 2015. Microbial hotspots and hot moments in soil: concept & review. Soil Biology and Biochemistry 83, 184–199. https://doi.org/10.1016/j.soilbio.2015.01.025.

Kuzyakov, Y., Hill, P.W., Jones, D.L., 2007. Root exudate components change litter decomposition in a simulated rhizosphere depending on temperature. Plant and Soil 290, 293–305. https://doi.org/10.1007/s11104-006-9162-8.

Kuzyakov, Y., Razavi, B.S., 2019. Rhizosphere size and shape: temporal dynamics and spatial stationarity. Soil Biology and Biochemistry 135, 343–360. https://doi.org/10.1016/j.soilbio.2019.05.011.

Li, C., Ding, S., Yang, L., Zhu, Q., Chen, M., Tsang, D.C.W., Cai, G., Feng, C., Wang, Y., Zhang, C., 2019. Planar optode: a two-dimensional imaging technique for studying spatial-temporal dynamics of solutes in sediment and soil. Earth-Science Reviews 197, 102916. https://doi.org/10.1016/j.earscirev.2019.102916.

Lipson, D.A., 2015. The complex relationship between microbial growth rate and yield and its implications for ecosystem processes. Frontiers in Microbiology 6. https://doi.org/10.3389/fmicb.2015.00615.

Liu, Q., Xu, X., Wang, H., Blagodatskaya, E., Kuzyakov, Y., 2019. Dominant extracellular enzymes in priming of SOM decomposition depend on temperature. Geoderma 343, 187–195. https://doi.org/10.1016/j.geoderma.2019.02.006.

Luli, G.W., Strohl, W.R., 1990. Comparison of growth, acetate production, and acetate inhibition of Escherichia coli strains in batch and fed-batch fermentations. Applied and Environmental Microbiology 56, 1004–1011. https://doi.org/10.1128/aem.56.4.1004-1011.1990.

Luo, Z., Wang, E., Sun, O.J., 2016. A meta-analysis of the temporal dynamics of priming soil carbon decomposition by fresh carbon inputs across ecosystems. Soil Biology and Biochemistry 101, 96–103. https://doi.org/10.1016/j.soilbio.2016.07.011.

Manzoni, S., Porporato, A., 2009. Soil carbon and nitrogen mineralization: theory and models across scales. Soil Biology and Biochemistry 41, 1355–1379. https://doi.org/10.1016/j.soilbio.2009.02.031.

Mau, R.L., Liu, C.M., Aziz, M., Schwartz, E., Dijkstra, P., Marks, J.C., Price, L.B., Keim, P., Hungate, B.A., 2015. Linking soil bacterial biodiversity and soil carbon stability. The ISME Journal 9, 1477–1480. https://doi.org/10.1038/ismej.2014.205.

Mondini, C., Cayuela, M.L., Sanchez-Monedero, M.A., Roig, A., Brookes, P.C., 2006. Soil microbial biomass activation by trace amounts of readily available substrate. Biology and Fertility of Soils 42, 542–549. https://doi.org/10.1007/s00374-005-0049-2.

Mori, M., Marinari, E., De Martino, A., 2019. A yield-cost tradeoff governs Escherichia coli's decision between fermentation and respiration in carbon-limited growth. Npj Systems Biology and Applications 5, 16. https://doi.org/10.1038/s41540-019-0093-4.

Murphy, C.J., Baggs, E.M., Morley, N., Wall, D.P., Paterson, E., 2015. Rhizosphere priming can promote mobilisation of N-rich compounds from soil organic matter. Soil Biology and Biochemistry 81, 236–243. https://doi.org/10.1016/j.soilbio.2014.11.027.

Murray, P., Ostle, N., Kenny, C., Grant, H., 2004. Effect of defoliation on patterns of carbon exudation from Agrostis capillaris. Journal of Plant Nutrition and Soil Science 167, 487–493. https://doi.org/10.1002/jpln.200320371.

Nannipieri, P., Eldor, P., 2009. The chemical and functional characterization of soil N and its biotic components. Soil Biology and Biochemistry 41, 2357–2369. https://doi.org/10.1016/j.soilbio.2009.07.013.

Nottingham, A.T., Turner, B.L., Chamberlain, P.M., Stott, A.W., Tanner, E.V.J., 2012. Priming and microbial nutrient limitation in lowland tropical forest soils of contrasting fertility. Biogeochemistry 111, 219–237.

Oyewole, O.A., Inselsbacher, E., Näsholm, T., 2014. Direct estimation of mass flow and diffusion of nitrogen compounds in solution and soil. New Phytologist 201, 1056–1064. https://doi.org/10.1111/nph.12553.

Papp, K., Hungate, B.A., Schwartz, E., 2020. Glucose triggers strong taxon-specific responses in microbial growth and activity: insights from DNA and RNA qSIP. Ecology 101, 1–12. https://doi.org/10.1002/ecy.2887.

Pfeiffer, T., Bonhoeffer, S., 2003. An evolutionary scenario for the transition to undifferentiated multicellularity. Proceedings of the National Academy of Sciences 100, 1095–1098. https://doi.org/10.1073/pnas.0335420100.

Pfeiffer, T., Schuster, S., Bonhoeffer, S., 2001. Cooperation and competition in the evolution of ATP-producing pathways. Science 292, 504–507. https://doi.org/10.1126/science.1058079.

Phillips, R.L., Zak, D.R., Holmes, W.E., White, D.C., 2002. Microbial community composition and function beneath temperate trees exposed to elevated atmospheric carbon dioxide and ozone. Oecologia 131, 236–244. https://doi.org/10.1007/s00442-002-0868-x.

R Core Team, 2022. R: A Language and Environment for Statistical Computing. R Foundation for Statistical Computing, Vienna, Austria [WWW Document]. URL. https://www.r-project.org/.

Santner, J., Larsen, M., Kreuzeder, A., Glud, R.N., 2015. Two decades of chemical imaging of solutes in sediments and soils – a review. Analytica Chimica Acta 878, 9–42. https://doi.org/10.1016/j.aca.2015.02.006.

Sauer, D., Kuzyakov, Y., Stahr, K., 2006. Spatial distribution of root exudates of five plant species as assessed by 14C labeling. Journal of Plant Nutrition and Soil Science 169, 360–362. https://doi.org/10.1002/jpln.200621974.

Schimel, J.P., Weintraub, M.N., 2003. The implications of exoenzyme activity on microbial carbon and nitrogen limitation in soil: a theoretical model. Soil Biology and Biochemistry 35, 549–563. https://doi.org/10.1016/S0038-0717(03)00015-4.

Schink, S.J., Christodoulou, D., Mukherjee, A., Athaide, E., Brunner, V., Fuhrer, T., Bradshaw, G.A., Sauer, U., Basan, M., 2022. Glycolysis/gluconeogenesis specialization in microbes is driven by biochemical constraints of flux sensing. Molecular Systems Biology 18. https://doi.org/10.15252/msb.202110704.

Seitz, V.A., McGivern, B.B., Daly, R.A., Chaparro, J.M., Borton, M.A., Sheflin, A.M., Kresovich, S., Shields, L., Schipanski, M.E., Wrighton, K.C., Prenni, J.E., 2022. Variation in root exudate composition influences soil microbiome membership and function. Applied and Environmental Microbiology 88. https://doi.org/10.1128/aem.00226-22.

Shi, S., Richardson, A.E., O'Callaghan, M., DeAngelis, K.M., Jones, E.E., Stewart, A., Firestone, M.K., Condron, L.M., 2011. Effects of selected root exudate components on soil bacterial communities. FEMS Microbiology Ecology 77, 600–610. https://doi.org/10.1111/j.1574-6941.2011.01150.x.

Smith, W.H., 1976. Character and significance of forest tree root exudates. Ecology 57, 324–331. https://doi.org/10.2307/1934820.

Song, W., Hu, C., Luo, Y., Clough, T.J., Wrage-Mönnig, N., Ge, T., Luo, J., Zhou, S., Qin, S., 2023. Nitrate as an alternative electron acceptor destabilizes the mineral associated organic carbon in moisturized deep soil depths. Frontiers in Microbiology 14. https://doi.org/10.3389/fmicb.2023.1120466.

Spohn, M., Carminati, A., Kuzyakov, Y., 2013. Soil zymography – a novel in situ method for mapping distribution of enzyme activity in soil. Soil Biology and Biochemistry 58, 275–280. https://doi.org/10.1016/j.soilbio.2012.12.004.

Szenk, M., Dill, K.A., De Graff, A.M.R., 2017. Why do fast-growing bacteria enter overflow metabolism? Testing the membrane real estate hypothesis. Cell Systems 5, 95–104. https://doi.org/10.1016/j.cels.2017.06.005.

Takaya, N., 2002. Dissimilatory nitrate reduction metabolisms and their control in fungi. Journal of Bioscience and Bioengineering 94, 506–510. https://doi.org/10.1016/S1389-1723(02)80187-6.

Vetterlein, D., Carminati, A., Kögel-Knabner, I., Bienert, G.P., Smalla, K., Oburger, E., Schnepf, A., Banitz, T., Tarkka, M.T., Schlüter, S., 2020. Rhizosphere spatiotemporal organization–A key to rhizosphere functions. Frontiers in Agronomy 2, 1–22. https://doi.org/10.3389/fagro.2020.00008.

Vives-Peris, V., de Ollas, C., Gómez-Cadenas, A., Pérez-Clemente, R.M., 2020. Root exudates: from plant to rhizosphere and beyond. Plant Cell Reports 39, 3–17. https://doi.org/10.1007/s00299-019-02447-5.

Vogel, C., Mueller, C.W., Höschen, C., Buegger, F., Heister, K., Schulz, S., Schloter, M., Kögel-Knabner, I., 2014. Submicron structures provide preferential spots for carbon and nitrogen sequestration in soils. Nature Communications 5, 1–7. https://doi.org/10.1038/ncomms3947.

Voltolini, M., Taş, N., Wang, S., Brodie, E.L., Ajo-Franklin, J.B., 2017. Quantitative characterization of soil micro-aggregates: new opportunities from sub-micron resolution synchrotron X-ray microtomography. Geoderma 305, 382–393. https://doi.org/10.1016/j.geoderma.2017.06.005.

Warren, C.R., 2018. Development of online microdialysis-mass spectrometry for continuous minimally invasive measurement of soil solution dynamics. Soil Biology and Biochemistry 123, 266–275. https://doi.org/10.1016/j.soilbio.2018.05.022.

Wenzel, W.W., Wieshammer, G., Fitz, W.J., Puschenreiter, M., 2001. Novel rhizobox design to assess rhizosphere characteristics at high spatial resolution. Plant and Soil 237, 37–45. https://doi.org/10.1023/A:1013395122730.

Wickham, H., 2016. ggplot2: Elegant Graphics for Data Analysis. Springer-Verlag, New York.

Wild, B., Schnecker, J., Alves, R.J.E., Barsukov, P., Bárta, J., Čapek, P., Gentsch, N., Gittel, A., Guggenberger, G., Lashchinskiy, N., Mikutta, R., Rusalimova, O., Šantrůčková, H., Shibistova, O., Urich, T., Watzka, M., Zrazhevskaya, G., Richter, A., 2014. Input of easily available organic C and N stimulates microbial decomposition of soil organic matter in arctic permafrost soil. Soil Biology and Biochemistry 75, 143–151. https://doi.org/10.1016/j.soilbio.2014.04.014.

Willers, C., Jansen van Rensburg, P.J., Claassens, S., 2015. Phospholipid fatty acid profiling of microbial communities-a review of interpretations and recent applications. Journal of Applied Microbiology 119, 1207–1218. https://doi.org/10.1111/jam.12902.

Wolfe, A.J., 2005. The acetate switch. Microbiology and Molecular Biology Reviews 69, 12–50. https://doi.org/10.1128/MMBR.69.1.12-50.2005.

Wortel, M.T., Noor, E., Ferris, M., Bruggeman, F.J., Liebermeister, W., 2018. Metabolic enzyme cost explains variable trade-offs between microbial growth rate and yield. PLoS Computational Biology 14, e1006010. https://doi.org/10.1371/journal.pcbi.1006010.

Zhalnina, K., Louie, K.B., Hao, Z., Mansoori, N., da Rocha, U.N., Shi, S., Cho, H., Karaoz, U., Loqué, D., Bowen, B.P., Firestone, M.K., Northen, T.R., Brodie, E.L., 2018. Dynamic root exudate chemistry and microbial substrate preferences drive patterns in rhizosphere microbial community assembly. Nature Microbiology 3, 470–480. https://doi.org/10.1038/s41564-018-0129-3.

Zhu, B., Gutknecht, J.L.M.M., Herman, D.J., Keck, D.C., Firestone, M.K., Cheng, W., 2014. Rhizosphere priming effects on soil carbon and nitrogen mineralization. Soil Biology and Biochemistry 76, 183–192. https://doi.org/10.1016/j.soilbio.2014.04.033.

zu Schweinsberg-Mickan, M.S., Joergensen, R.G., Müller, T., 2010. Fate of 13C- and 15N-labelled rhizodeposition of Lolium perenne as function of the distance to the root surface. Soil Biology and Biochemistry 42, 910–918. https://doi.org/10.1016/j.soilbio.2010.02.007.